PHYSICAL REVIEW D **90,** 044024 (2014)

Phase structure of cold magnetized quark matter within the SU(3) NJL model

Ana G. Grunfeld,[1,2] Débora P. Menezes,[3,4] Marcus B. Pinto,[3] and Norberto N. Scoccola[1,2,5]

[1]*CONICET, Rivadavia 1917, 1033 Buenos Aires, Argentina*
[2]*Department of Theoretical Physics, Comisión Nacional de Energía Atómica, Avenida Libertador 8250, 1429 Buenos Aires, Argentina*
[3]*Departamento de Física CFM, Universidade Federal de Santa Catarina, Florianópolis, SC, CEP 88.040-900, Brazil*
[4]*Departamento de Física Aplicada, Universidad de Alicante, E-03080, Alicante, Spain*
[5]*Universidad Favaloro, Solís 453, 1078 Buenos Aires, Argentina*

(Received 21 February 2014; published 12 August 2014)

The possible different phases of homogeneous cold quark matter in the presence of a finite magnetic field and chemical potential are obtained within the SU(3) NJL model for two parameter sets often used in the literature. Although the general pattern is the same in both cases, the number of intermediate phases is parameter dependent. The chiral susceptibilities, as usually defined, are different not only for the s quark as compared with the two light quarks, but also for the u and d quarks, yielding nonidentical crossover lines for the light quark sector. The results for stellar matter, imposing charge neutrality and β equilibrium, are also presented for the same sets of parameters. The corresponding phase diagrams show some differences with respect to the symmetric cases. It is found that for stellar matter the inverse catalysis effect is less pronounced and the transition to the fully chiral symmetry-restored phase occurs at higher chemical potentials.

DOI: 10.1103/PhysRevD.90.044024 PACS numbers: 24.10.Jv, 25.75.Nq

I. INTRODUCTION

The study of the QCD phase diagram, when matter is subject to intense external magnetic fields, has been recently a topic of intense investigation. The fact that magnetic fields can reach intensities of the order of $B \sim 10^{19}$ G or higher in heavy-ion collisions [1] and up to 10^{18} G in the center of magnetars [2,3] made theoretical physicists consider matter subject to a magnetic field both at high temperatures and low densities and low temperatures and high densities. The majority of the effective models foresee that at zero chemical potential a crossover transition is obtained at a pseudocritical temperature, $T_{\rm pc}$, that increases with an increasing magnetic field, a behavior that is contrary to the one found in lattice QCD (LQCD) calculations [4–6]. Possible physical explanations for this discrepancy have been recently given in Refs. [7–9]. The physical arguments are mostly based on the fact that in quark effective models some effects are missing due, for instance, to the indirect interaction between the gluons and the magnetic field via quark exchange. Such a backreaction is naturally implemented in the so-called entangled Polyakov-Nambu-Jona-Lasinio model (EPNJL) [10] in which the four-quark coupling of the Nambu-Jona-Lasinio model (NJL) [11] is considered to be dependent on the Polyakov loop. Although such a model is also unable [12] to produce inverse magnetic catalysis (IMC), a very recent study [13] has shown the existence of such effect. In those studies, the lattice data are fitted under the assumption that the pure gauge-critical temperature T_0 (a parameter in the NJL model) is a function of the magnetic field. The four-quark coupling of the NJL model has also been taken to depend on B [14] in a way that mimics the asymptotic behavior similar to the one displayed by the QCD coupling [15]. In this case, the model can also predict a decrease of $T_{\rm pc}$ with B in accordance with the LQCD findings.

As LQCD calculations are not yet in position to describe the whole T-μ plane, further investigations with effective models have been developed toward a better understanding of the behavior of the quark condensates [13], in the search for coexistent chemical potentials at subcritical temperatures [16] as well as the existence and possible location of the critical end point [16,17]. In the case of magnetized quark matter, some interesting results were obtained from these investigations. Namely, the first-order segment of the transition line becomes longer as the field strength increases so that a larger coexistence region for hadronic and quark matter should be expected for strong magnetic fields affecting the position of the (second-order) critical point where the first-order transition line terminates.

In Ref. [16], it was observed that at subcritical temperatures the coexistence chemical potential (μ_c) decreases with increasing values of the magnetic fields in a manifestation of the IMC effect described in Ref. [18] where it is argued that this phenomenon should be generally observed at low temperatures in a model-independent way. Therefore, although the results of the extension of the NJL model at high temperatures and vanishing density do not seem to agree

with the lattice predictions unless one implements some of the prescriptions given in Refs. [13,14], one feels more confident about the correctness of the IMC observed at low temperatures and high densities with effective models where perhaps the backreaction is less important. We refer the reader to Ref. [18] for a physically intuitive discussion of the IMC phenomenon.

Note that the IMC can be reversed when extremely high fields are considered so that μ_c oscillates around the B = 0 value for magnetic fields within the 10^{17}–10^{20} G range. However, one has to bear in mind that these values are above the cutoff scale [16]. Together, all of these effects have interesting consequences for quantities that depend on the details of the coexistence region such as the surface tension, as recently discussed in Ref. [19]. It is also worth remarking that other physical possibilities such as the isospin and strangeness content of the system, the presence of a vector interaction [20], and the adopted model approximation within a particular parametrization may influence these results mostly in a quantitative way.

As it is well known, in the absence of a magnetic field dynamical chiral symmetry breaking (DCSB) occurs, within four fermion theories, when the coupling (G) exceeds a critical value (G_c), at least in the 2 + 1 d and 3 + 1 d cases. However, when $B \neq 0$, DCSB may occur even when the coupling is smaller than G_c. This effect, which is related to a dimensional reduction induced by B, is known as magnetic catalysis (MC). It was first observed in Refs. [21,22] and then explained in Ref. [23] (see Ref. [24] for recent reviews). Following its discovery, Ebert *et al.* [25] recognized that MC associated to the filling of Landau levels (LLs) could lead to more exotic phase transition patterns as a consequence of the induced magnetic oscillations. To confirm this assumption, these authors have considered a wide range of coupling values for the two flavor NJL model in the chiral case [11]. As expected, they have observed many phase structures as a function of the chemical potential: an infinite number of massless chirally symmetric phases, a cascade of massive phases with broken chiral invariance and tricritical points were also obtained. Recently, these seminal works have been extended by a more systematic and numerically accurate analysis of the two flavor case considering different model parametrizations identified by the vacuum value of the dressed quark mass M_0 in the absence of an external magnetic field [26]. In that reference, other relevant physical quantities, such as susceptibilities, have been considered in order to produce a phase diagram for cold magnetized quark matter. Although the more complex transition patterns show up for rather low values of the dressed quark mass $M_0 \simeq 200$ MeV, even with more canonical values of the model parameters leading to $M_0 \simeq 300$–400 MeV, more than one first-order phase transition, which is signaled when the thermodynamical potential develops two degenerate minima at different values of the coexistence chemical potential, is found. We point out that this fact has also been recently observed to arise within another effective four-fermion theory described by the 2 + 1 d Gross-Neveu model [27]. In general, *weak* first-order transitions can be easily missed in a numerical evaluation due to the fact that the two degenerate minima appear almost at the same location being separated by a tiny potential barrier so that their study requires extra care. Physically, this corresponds to a situation where two different (but almost identical) densities coexist at the same chemical potential, temperature, and pressure. Also, since these shallow minima are separated by a low potential barrier, one may also expect the surface tension to be small in this case [28].

At this point, it is important to recall that strangeness is generally believed to be of great relevance for the physics of quark stars and the heavy ion collisions and hence cannot be disregarded. For instance, in astrophysical applications, the magnetic oscillations studied in Refs. [25,26] may influence the equation of state, which is the starting point as far as the prediction of observables, such as the mass and radius of a compact star, is concerned. Therefore, as a step toward the full understanding of the role played by strangeness in these physical situations, in the present work, we extend the detailed analysis of cold quark matter recently performed with the two-flavor version to the three-flavor version of the NJL model, which is described in terms of two canonical sets of input parameters. At the same time, charge neutrality and β equilibrium are essential conditions in understanding the behavior of quark matter subject to strong magnetic fields [3] in the study of magnetars. Moreover, the existence and location of the critical end point are related to the amount of different quark flavors in the system [17], which influences the whole phase diagram. Therefore, in the present work, we also consider the effects of charge neutrality and β equilibrium besides strangeness.

In the next section, we show the necessary formalism used to describe quark matter under strong magnetic fields with the three-flavor NJL, and in Sec. III, we present our numerical results. Our final remarks are presented in Sec. IV.

II. FORMALISM

We consider the SU(3) NJL Lagrangian density, which includes a scalar-pseudoscalar interaction and the t'Hooft six-fermion interaction [29] in the presence of an external magnetic field and chemical potential, and it is written as

$$\mathcal{L} = \bar{\psi}(iD - \hat{m}_c + \hat{\mu}\gamma^0)\psi + G\sum_{a=0}^{8}[(\bar{\psi}\lambda_a\psi)^2 + (\bar{\psi}i\gamma_5\lambda_a\psi)^2] - K(d_+ + d_-), \quad (1)$$

where G and K are coupling constants, $\psi = (u, d, s)^T$ represents a quark field with three flavors, $d_\pm = \det[\bar{\psi}(1 \pm \gamma_5)\psi]$, $\hat{\mu} = \mathrm{diag}(\mu_u, \mu_d, \mu_s)$ the quark chemical potentials, $\hat{m}_c = \mathrm{diag}(m_u, m_d, m_s)$ is the corresponding (current) mass matrix, $\lambda_0 = \sqrt{2/3}I$, where I is the unit matrix in the three-flavor space, and $0 < \lambda_a \leq 8$ denote the Gell-Mann matrices. The coupling of the quarks to the

electromagnetic field $\mathcal{A}_\mu$ is implemented through the covariant derivative $D_\mu = \partial_\mu - i\hat{q}\mathcal{A}_\mu$ where $\hat{q}$ represents the quark electric charge matrix $\hat{q} = \mathrm{diag}(q_u, q_d, q_s)$ where $q_u/2 = -q_d = -q_s = e/3$. In the present work, we consider a static and constant magnetic field in the z direction, $\mathcal{A}_\mu = \delta_{\mu 2} x_1 B$. In the mean-field approximation the Lagrangian density [Eq. (1)] can be written as [3]

$$\mathcal{L}^{\mathrm{MFA}} = \bar{\psi}(iD - \hat{M} + \hat{\mu}\gamma^0)\psi - 2G(\phi_u^2 + \phi_d^2 + \phi_s^2) + 4K\phi_u\phi_d\phi_s, \tag{2}$$

where $\hat{M} = \mathrm{diag}(M_u, M_d, M_s)$ is a matrix with elements defined by the dressed quark masses which satisfy the set of three coupled gap equations:

$$\begin{aligned} f_u(M_u, M_d, M_s) &= M_u - m_u + 4G\phi_u - 2K\phi_d\phi_s = 0, \\ f_d(M_u, M_d, M_s) &= M_d - m_d + 4G\phi_d - 2K\phi_s\phi_u = 0, \\ f_s(M_u, M_d, M_s) &= M_s - m_s + 4G\phi_s - 2K\phi_u\phi_d = 0. \end{aligned} \tag{3}$$

In Eqs. (2) and (3), ϕ_f is the quark condensate associated to each flavor which contains three different terms: the vacuum, the magnetic, and the in-medium one. At vanishing temperatures, these contributions read

$$\phi_f = \langle\bar{\psi}_f\psi_f\rangle = \phi_f^{\mathrm{vac}} + \phi_f^{\mathrm{mag}} + \phi_f^{\mathrm{med}}, \tag{4}$$

where

$$\begin{aligned} \phi_f^{\mathrm{vac}} &= -\frac{N_c M_f}{2\pi^2}\left[\Lambda\sqrt{\Lambda^2 + M_f^2} - M_f^2 \ln\left(\frac{\Lambda + \sqrt{\Lambda^2 + M_f^2}}{M_f}\right)\right], \\ \phi_f^{\mathrm{mag}} &= -\frac{N_c M_f |q_f| B}{2\pi^2}\left[\ln\Gamma(x_f) - \frac{1}{2}\ln(2\pi) + x_f - \frac{1}{2}(2x_f - 1)\ln(x_f)\right], \\ \phi_f^{\mathrm{med}} &= \frac{N_c}{2\pi^2} M_f |q_f| B \sum_{\nu=0}^{\nu_f^{\max}} \alpha_\nu \ln\left(\frac{\mu_f + \sqrt{\mu_f^2 - s_f(\nu, B)^2}}{s_f(\nu, B)}\right), \end{aligned} \tag{5}$$

where $s_f(\nu, B) = \sqrt{M_f^2 + 2|q_f|B\nu}$, Λ represents a noncovariant ultraviolet cutoff [25], while $x_f = M_f^2/(2|q_f|B)$ and μ_f are the quark chemical potentials for each flavor. We note at this stage that when dealing with extensions of the present model that include color pairing interactions it has become customary [30] to introduce some soft regulator function to avoid the unphysical oscillations induced by the use of a sharp cutoff in the magnetic-dependent terms. However, in the present situation, one can follow the procedure discussed in Ref. [3] in which only the vacuum term needs to be regularized. In this way, the presence of the above-mentioned oscillations can be avoided even when a noncovariant sharp cutoff term is used to regulate it. In ϕ_f^{med}, the sum is over the LLs represented by ν, while $\alpha_\nu = 2 - \delta_{\nu 0}$ is a degeneracy factor and $\nu_f^{\max}$ is the largest integer that satisfies $\nu_f^{\max} \leq (\mu_f^2 - M_f^2)/(2|q_f|B)$.

Then, within the mean-field approximation, the grand-canonical thermodynamical potential for cold and dense strange quark matter in the presence of an external magnetic field can be written as

$$\Omega = -(\theta_u + \theta_d + \theta_s) + 2G(\phi_u^2 + \phi_d^2 + \phi_s^2) - 4K\phi_u\phi_d\phi_s, \tag{6}$$

where θ_f gives the contribution from the gas of quasiparticles and can be written as the sum of three contributions,

$$\begin{aligned} \theta_f^{\mathrm{vac}} &= -\frac{N_c}{8\pi^2}\left[M_f^4 \ln\left(\frac{\Lambda + \sqrt{\Lambda^2 + M_f^2}}{M_f}\right) - \sqrt{\Lambda^2 + M_f^2}\Lambda(2\Lambda^2 + M_f^2)\right], \\ \theta_f^{\mathrm{mag}} &= \frac{N_c}{2\pi^2}(|q_f|B)^2\left[\zeta^{(1,0)}(-1, x_f) - \frac{1}{2}(x_f^2 - x_f)\ln x_f + \frac{x_f^2}{4}\right], \\ \theta_f^{\mathrm{med}} &= \frac{N_c}{4\pi^2}|q_f|B\sum_{\nu=0}^{\nu_f^{\max}}\alpha_\nu\left[\mu_f\sqrt{\mu_f^2 - s_f(\nu, B)^2} - s_f(\nu, B)^2\ln\left(\frac{\mu_f + \sqrt{\mu_f^2 - s_f(\nu, B)^2}}{s_f(\nu, B)}\right)\right], \end{aligned} \tag{7}$$

TABLE I. Parameter sets for the NJL SU(3) model.

Parameter set	Λ MeV	$G\Lambda^2$	$K\Lambda^5$	$m_{u,d}$ MeV	m_s MeV
Set 1 [31]	631.4	1.835	9.29	5.5	135.7
Set 2 [32]	602.3	1.835	12.36	5.5	140.7

where $\zeta^{(1,0)}(-1, x_f) = d\zeta(z, x_f)/dz|_{z=-1}$ with $\zeta(z, x_f)$ being the Riemann-Hurwitz zeta function.

In our calculations, we first consider the simpler case of symmetric matter where all three quarks carry the same chemical potential μ. Afterward, we analyze the case of stellar matter in which leptons are also present and β equilibrium and charge neutrality are imposed. In this case, the chemical potential for each quark, μ_f, is a function of μ and the lepton chemical potentials which have to be self-consistently determined. In addition, in order to analyze the dependence of the results on the model parameters, we consider two widely used SU(3) NJL model parametrizations. Set 1 corresponds to that used in Ref. [31], while Set 2 corresponds to that of Ref. [32]. The corresponding model parameters are listed in Table I.

We end this section by describing the procedure used to identify the boundaries between the possible different phases of the magnetized quark matter. Namely, to obtain the critical chemical potential at given eB, we proceed as follows. In the case of first-order phase transitions, we have used the same prescription as in [16]; i.e., we have calculated the thermodynamical potential as a function of the dressed quark masses and then searched for two degenerate minima. In the case of crossover transitions, its position is identified by the peak of the chiral susceptibility. However, different from the standard SU(2) NJL model with maximum flavor mixing, within the present version of the SU(3) NJL model, the u and d dressed quark masses, as well as the corresponding condensates, are not necessarily the same. For this reason, we have defined different susceptibilities for each flavor $\chi_f = d\phi_f/dm_f$. The peak of these susceptibilities is used in the next sections to identify possible crossover transitions.

III. RESULTS FOR SYMMETRIC QUARK MATTER

In this section, we present and analyze the results of our numerical investigations for the case of symmetric quark matter. These were performed by solving the set of three coupled gap equations given in Eq. (3) for different values of the chemical potential $\mu = \mu_u = \mu_d = \mu_s$ and magnetic fields.

It should be noticed that, contrary to what happens in the case of the standard SU(2) NJL model with maximum flavor mixing [11,26], for these parametrizations, the difference between the u and d quark electric charges induces a splitting between the u and d dressed quark masses. Nonetheless, we have found that, in general, this splitting is quite small. Of course, due to the larger value of the associated current quark mass, M_s is always larger than M_u and M_d.

We stress that, for a given value of μ and B, the set of coupled gap equations might have several solutions. Obviously, the stable solution is the one that leads to the lowest value of the thermodynamical potential Eq. (7). Therefore, it is important to make sure that one does not miss any relevant solution when solving Eq. (3). In order to do that, we have proceeded as follows: given a value of M_u, the set of equations $\{f_d, f_s\}$ was used to numerically determine the corresponding values of M_d and M_s. These values were then inserted in the remaining gap equation that could be now considered as a function of the single variable M_u, i.e., $f_u[(M_u, M_d(M_u), M_s(M_u))]$. By varying M_u within a conveniently selected range of values, one could at this point determine all of the solutions of the coupled system of gap equations by finding all of the values of M_u at which this function vanishes. Of course, one has to be careful with a possible caveat that this method can have: it could happen that for a given value of M_u, the set of equations $\{f_d, f_s\}$ might have more than one solution. We have verified that, for the model parametrizations used in this work, which imply a rather strong flavor mixing leading to $M_u \approx M_d$, this situation did not arise for any of the values of μ and B considered.

We start by analyzing the behavior of the quark constituent masses as functions of the chemical potential for several representative values of the magnetic field shown as in Fig. 1. Note that here and in what follows we use natural units recalling the reader that $eB = 1$ GeV^2 corresponds to $B = 1.69 \times 10^{20}$ G. We consider first the situation for Set 1 (left panels) starting by the lowest chosen value of magnetic field $eB = 0.01$ GeV^2 (full red line). As we increase μ, we see that up to certain value $\mu_{c1} = 335.3$ MeV the dressed masses stay constant. At that point, we can observe a (tiny) sudden drop in the masses corresponding to a first-order phase transition which goes from the fully chirally broken phase, where the masses are μ independent, to a less massive one where the masses are μ dependent. As we continue to increase the chemical potential, there is a second tiny jump in the masses (somewhat more easily observed in the plot for M_d) at $\mu_{c2} = 342.3$ MeV. Increasing μ further we reach $\mu_{c3} = 345.4$ MeV where a new, in this case much larger, drop in the masses occur. After this point, the dressed u- and d-quark masses are much smaller than their vacuum values, indicating that light quark sector is in the fully chirally restored phase, namely that if we were to set $m_u = m_d = 0$ (i.e., chiral case) the associated dressed masses would vanish. To identify the different phases, it is convenient to adopt the notation of Refs. [11,26]. Thus, the fully chirally broken phase in which the system is for $\mu < \mu_{c1}$ is denoted by B. The massive phases in which M_f depends on μ are denoted C_α phases, where α is a set of three integers each of which

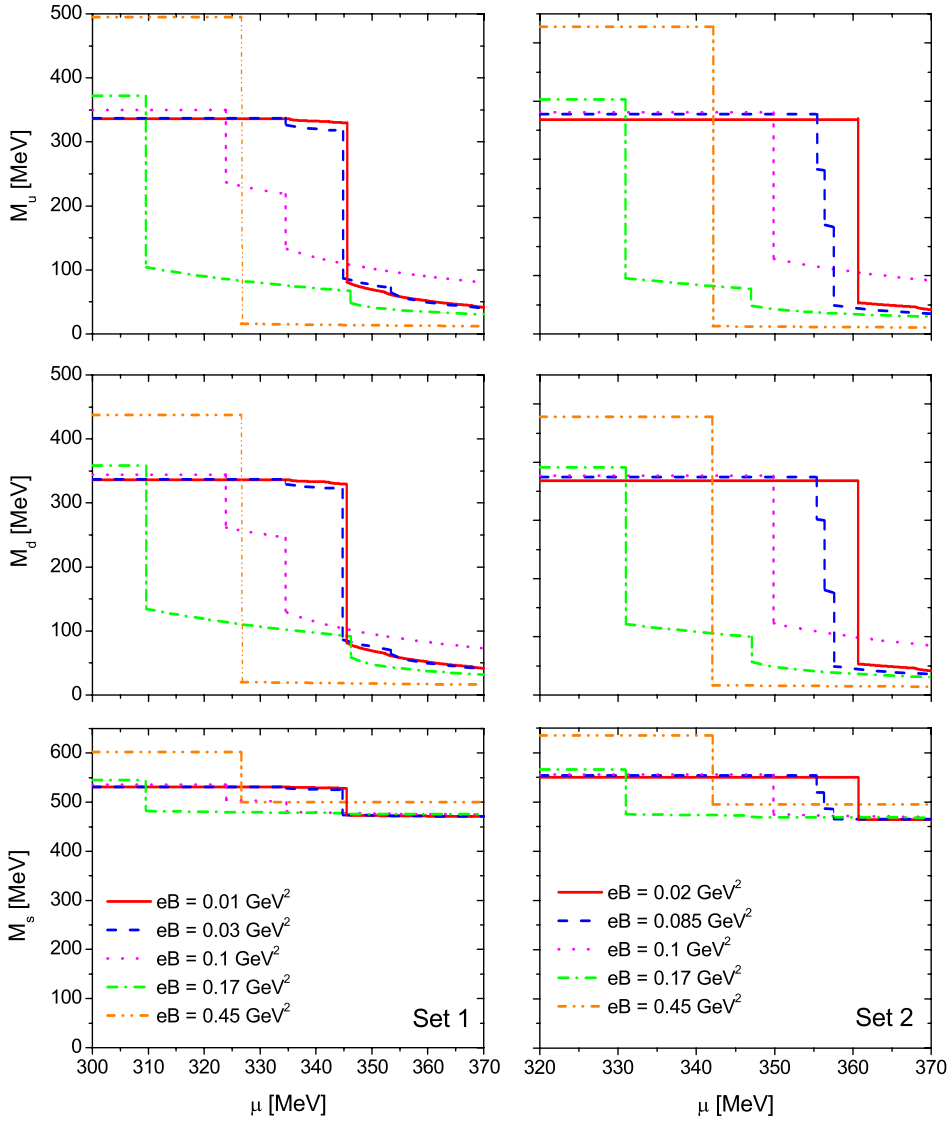

FIG. 1 (color online). Dressed quark masses as functions of chemical potential for different values of the magnetic field.

corresponds to the higher LL, which is populated for a given flavor. We note that within the range of values of the chemical potential considered in this work no s-quark LL is ever populated since this would require larger values of μ. Thus, in what follows, only two integers will be given, the first one corresponding to the u quark and the second to the d quark. Hence, the system is in the C_{00} phase if $\mu_{c1} < \mu_{c2}$ and in the C_{01} phase if $\mu_{c2} < \mu_{c3}$. The difference between these two phases is that in the C_{00} only the u-and d-quark lowest LLs (LLLs) are populated, while in C_{01} the d-quark first LL (1LL) also is populated. Moreover, the reason why the d-quark 1LL is populated without a simultaneous population of the u-quark 1LL is due to fact that $|q_d| = 2|q_u|$. For $\mu > \mu_{c3}$, the system is in one of the chirally restored phases A_α, where the difference between themselves is the number of light quark LLs that are populated. The transitions between these phases correspond to small jumps in the masses (i.e., first-order transitions), which in Fig. 1 are hardly seen in this case. Considering next case, $eB = 0.03$ GeV^2 (blue dashed line), we see that at basically the same value of μ_{c1} as the one given above, there is a first-order transition from the B phase to the C_{00} phase. However, in this case, no sign of a transition to the C_{01} phase is found as μ increases. In fact, the following transition corresponds to a big jump in the light quark dressed masses, which is associated to the transition between the C_{00} and one of the chiral symmetry restored phases A_α. It should be noted that this happens at a critical chemical potential which is slightly smaller than the value of μ_{c3} quoted above. As μ is further increased, consecutive first-order transitions between A_α occur. Note that the first of them can quite clearly be observed in this case. Turning to the case $eB = 0.10$ GeV^2 (magenta dotted lines), we see that the overall behavior is similar to that of $eB = 0.01$ GeV^2, except for the fact that in the present case the size of the first and second jumps in the masses are quite similar and that they occur at

lower values of μ. The situation for $eB = 0.17$ GeV^2 (green dash dotted lines) is somewhat peculiar. After a first large jump in the masses (occurring at an even lower value of μ than the previous cases), they decrease continuously for a rather wide interval of values of μ, which ends with a transition that is characteristic of those between A_α phases. Whether in that intermediate interval the system is always in the same phase (of A-type type) or it stays first in the C_{00} phase performing at some point a crossover transition to a A-type phase is a question that requires further analysis and is addressed below. Finally, for $eB = 0.45$ GeV^2 (orange dash dot dotted lines), the behavior of the system as μ increases becomes much simpler. There is one single first-order phase transition that connects the B and A_{00} phases. Note, however, that this transition occurs at a higher chemical potential as compared to that required in the previous case to induce a transition from the B phase. Turning our attention to the results concerning Set 2 (right panels in Fig. 1), we observe that although for $eB = 0.45$ GeV^2 (orange dash dot dotted lines) the behavior is very similar as the corresponding one for Set 1, at low values of eB there are significant differences. For example, for $eB = 0.02$ GeV^2 (full red lines), the first transition already connects the B phase with one of the A-type ones; i.e., there is no sign of an intermediate C_{00} here. As it turns out, such a phase only exists for a narrow interval of values of eB of which we take $eB = 0.085$ GeV^2 (dashed blue line) as a typical example.

In Fig. 2, we show the eB-μ phase diagrams obtained with both parameter sets. Note that in order to simplify the figure, we have introduced a compact notation to indicate the phases. In this way, the pair of integers mn corresponds to the C_{mn} phase and the pair $\bar{m}\,\bar{n}$ to the A_{mn} phase. Accordingly, the case to be discussed below in which one quark is in a C-type phase and the other in the A-type phase is indicated by putting a bar on top of the integer associated with the A-type phase. Thus, for example, $\bar{0}0$ corresponds to a region in which the u-quark sector is in the A-type phase and d-quark sector in the C-type phase. Note that in all of the cases $m = \mathrm{Int}[n/2]$. This follows from the relation between the light quark electric charges and the fact that we are dealing with symmetric matter with a rather strong flavor mixing. The full lines correspond to first-order phase transitions, while the dashed and dotted ones to smooth crossovers. As mentioned above, the later typically connect some of the C-type phases to a A-type one, and their determination requires a detailed analysis. In the first place, we should stress that, as well known, there is not a unique way to define a crossover transition. In the case of SU(2) cold quark matter under strong magnetic fields, this issue was discussed in some detail in Ref. [26]. Following that reference, we base our analysis on the chiral susceptibilities introduced at the end of the previous section. In particular, we define the crossover transition line as the ridge occurring in the chiral susceptibility when regarded as a two

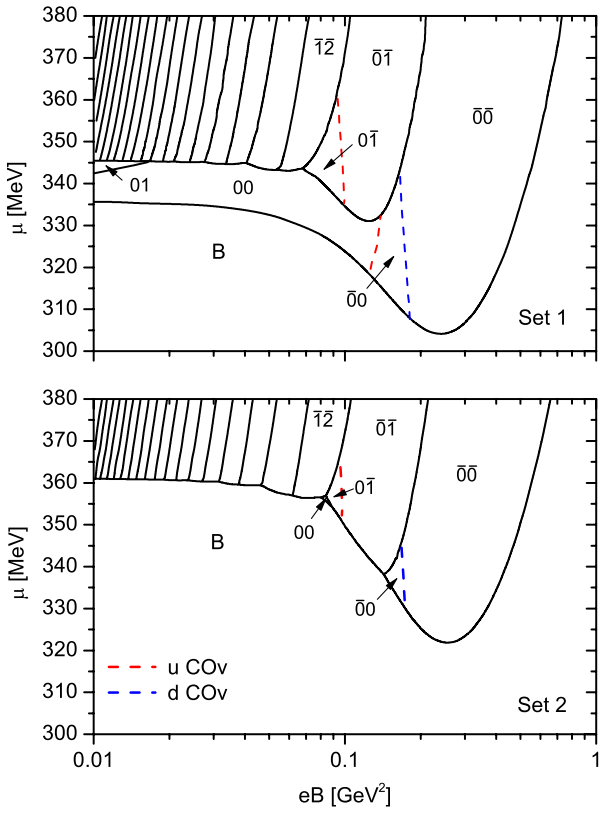

FIG. 2 (color online). Phase diagrams in the eB-μ for the set of parameters defined in Table I. As explained in the text, the pair of integers mn corresponds to the C_{mn} phase and the pair $\bar{m}\,\bar{n}$ to the A_{mn} phase. The case in which one quark is in a C-type phase and the other in the A-type phase is indicated by putting a bar on top of the integer associated with the A-type phase.

dimensional function of eB and μ. Mathematically, it can be defined by using for each value of the susceptibility (starting from its maximum value in the given region) the location of the points at which the gradient in the eB-μ plane is smaller. As remarked in Ref. [26], this definition must be complemented with the condition that on each side of the curve there should exist at least one region such that there is a maximum in the susceptibility for an arbitrary path connecting both regions. It is important to note that, different from the $SU(2)$ case discussed in that reference where one single chiral susceptibility can be defined for the two light flavors, the values of χ_u and χ_d at a given point in the eB-μ plane are in general different in the present case [33]. Therefore, there is no reason why there should be identical crossover lines for the two light quark sectors. In fact and in contrast to what happens with the first-order transitions which always coincide, the results of our analysis indicate that for the parametrizations considered this is never the case. As a consequence of this, there might be regions in the eB-μ plane where the u-quark sector is in a C-type phase and the d-quark sector in a A-type one or vice versa. For example, our results indicate the existence of a

$\bar{0}0$ phase for both model parametrizations. From Fig. 2 it is clear that the most remarkable difference between the phase diagrams associated to the two parametrizations considered concerns the regions in which the phases C_α exist. For Set 1, the C_{00} phase covers a rather large area of the plane, which in the eB direction extends from very low values up to $eB \simeq 0.15$ GeV^2 where it has a smooth crossover boundary with the phase A_{00}. Note that such a boundary is somewhat different for the two light quark sectors giving rise to an intermediate $\bar{0}0$ region. Moreover, for this parameter set, a small region of C_{01} phase exists for low values of eB. In the case of Set 2, however, the phase C_{00} only exists in a small triangular region surrounded by first-order transition lines, although a small $\bar{0}0$ region is also present. Another point that it is interesting to address regards the similarities between the present phase diagrams and those reported in Ref. [26] for the SU(2) case with maximum flavor mixing. In fact, the phase diagram obtained for Set 1 has strong similarities to that shown for $M_0 = 340$ MeV shown in Fig. 12 of that reference. Moreover, that of Set 2 appears to correspond to one somewhere in between those of $M_0 = 360$ MeV and $M_0 = 380$ MeV of that figure. Interestingly, the vacuum values of the u- and d-dressed quark masses in the vacuum and in the absence of a magnetic field are $M_u = M_d = 336(368)$ MeV for Set 1 (Set 2). Thus, it appears that even in the $SU(3)$ case under consideration, the general features of the eB-μ diagram are dictated to a great extent by the values of light quark dressed

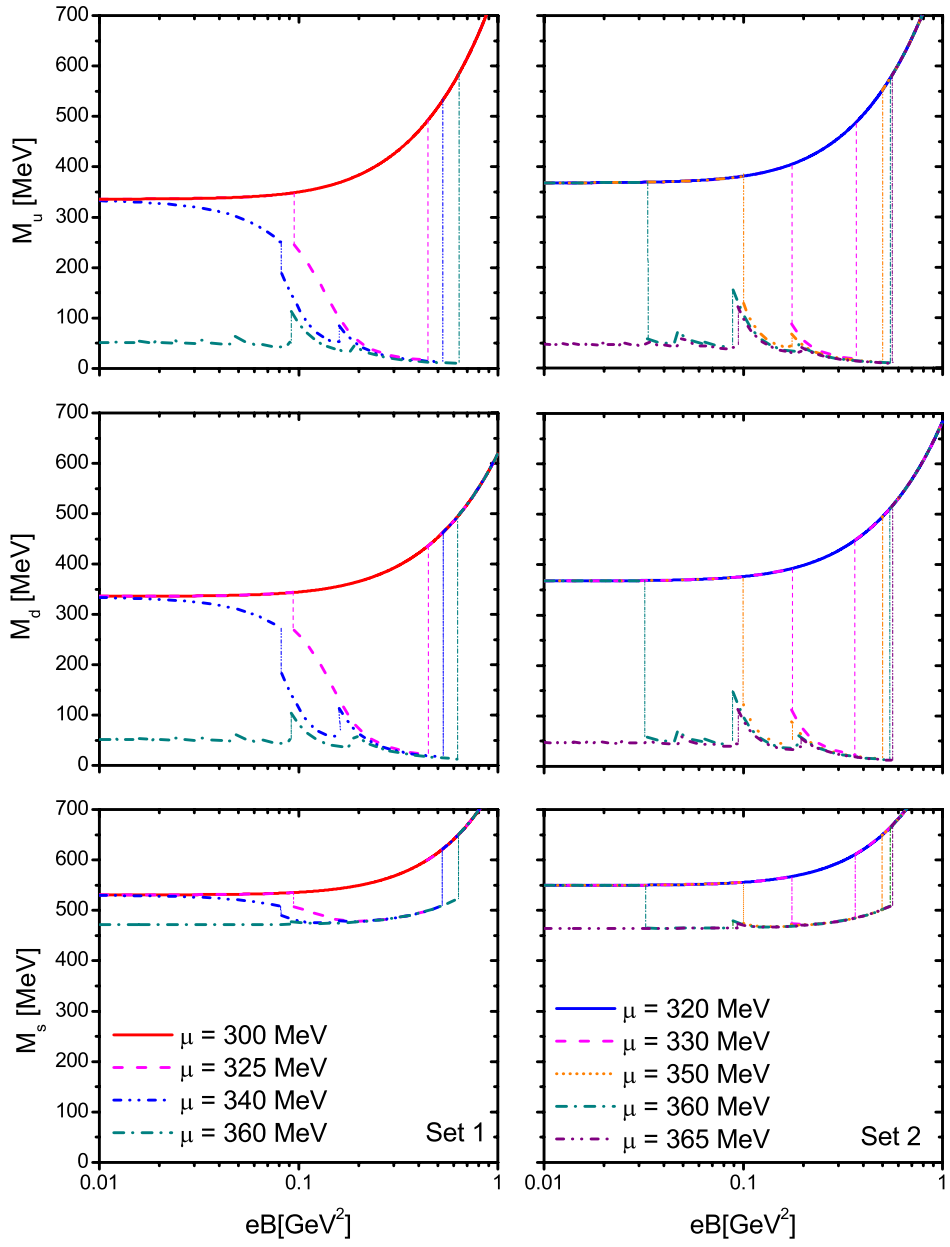

FIG. 3 (color online). Dressed quark masses as functions of magnetic field for different values of the chemical potential.

quark masses in the vacuum and in the absence of a magnetic field.

We end this section by analyzing in the context of the present SU(3) NJL model the MC effect mentioned in the Introduction and how this effect is modified by the presence of finite chemical potential leading, for example, to the existence of the so-called IMC. The later is usually related to a decrease of the critical chemical potential at intermediate values of the magnetic fields, an effect that can be understood in terms of extra cost in free energy to form a fermion-antifermion condensate at finite μ [18]. This extra cost originates in the LLL contribution to $\theta_f^{\rm med}$ in Eq. (7) which is linear in B and tends to decrease the difference in free energy between the vacuum phase and the finite density phase. Such a phenomenon is clearly observed in the phase diagrams displayed in Fig. 2. In fact, we see that after staying fairly constant up to $eB \simeq 0.05$ GeV^2 the lowest first-order transition line bends down, reaching a minimum at $eB \simeq 0.2$–0.3 GeV^2 after which it rises indefinitely with the magnetic field. This implies that, in general, there is some interval of values of the chemical potential for which an increase of the magnetic field at constant μ causes first a transition from the B-type phase to a one in which the light quarks are in a less massive phase (which could be either of C or A type) and afterward from the phase A_{00} back to massive phase B. To address these issues, we display in Fig. 3 the behavior of the masses as a function of magnetic fields for several chemical potentials and our two parameter sets. In particular, the complex phase structure for Set 1 (left panels) accounts for the different possible behaviors depending on the chemical potential. For $\mu = 300$ MeV (red full line), the system is in the B phase for the whole range of magnetic fields, and the MC effect is clearly seen. For $\mu = 325$ MeV (magenta dashed line), a similar behavior is seen, except for a middle section where the system passes through a C_{00} phase and an A_{00} phase before returning to the vacuum phase again. Note that when masses are plotted as functions of eB, the existence of a crossover transition from a C-type phase to A-type one becomes more noticeable. As already discussed, a detailed analysis shows that the associated critical magnetic field for u-quark sector is somewhat lower than that for d-quark sector. In this region of the curve, as well as in the rest of the following curves, the effect of IMC is also present. In fact, as already remarked in Ref. [26], we can conclude that within the C- and A-type phases the dressed light quark masses are basically decreasing functions of the magnetic field. This decrease has the same physical origin as the decrease of the critical chemical potential at intermediate values of the magnetic fields. In fact, it follows from the same contribution to the free energy. On the other hand, in the B phase, this contribution is not present, and thus, the usual MC effect takes place. In particular, for $\mu = 340$ MeV (blue dot dotted lines), the phase remains in C_{00} for a significant range of magnetic fields and the mass decreases continuously. Finally, for $\mu = 360$ MeV (green dash dotted lines) at low and medium magnetic fields, the system goes from a A_{mn} phase to another with $n' = n - 1$ as the magnetic fields increases, the transition between them being signaled by the peaks in the dressed masses. Recall that in the present case $m = \mathrm{Int}[n/2]$. Eventually, for sufficiently large magnetic fields, it has a first-order transition to the B phase. As shown in the right panels of Fig. 3, for Set 2, the situation is somewhat simpler. This is, of course, related to the absence of extended C_α regions in the associated phase diagram.

IV. RESULTS FOR STELLAR MATTER

In this section, we analyze the case of stellar matter, i.e., matter where β equilibrium and charge neutrality are imposed. In this case, electrons and muons are introduced into the system so that the thermodynamical potential receives an extra contribution [3]

$$\Omega^{\rm lep} = \sum_{l=e,\mu} \sum_{\nu=0}^{\nu_l^{\max}} \frac{|q_l| B \alpha_\nu}{4\pi^2} \left[\mu_l \sqrt{\mu_l^2 - s_l(\nu,B)^2} - s_l(\nu,B)^2 \ln\left(\frac{\mu_l + \sqrt{\mu_l^2 - s_l(\nu,B)^2}}{s_l(\nu,B)} \right) \right], \tag{8}$$

where $\nu_l^{\max} = \mathrm{Int}[(\mu_l^2 - m_l^2)/(2|q_l|B)]$ and $s_l(\nu,B) = \sqrt{m_l^2 + 2|q_l|B\nu}$. We take $m_e = 0.511$ MeV and $m_\mu = 105.66$ MeV.

β equilibrium and charge neutrality conditions are required and they are respectively given by

$$\mu_s = \mu_d = \mu_u + \mu_e, \qquad \mu_e = \mu_\mu \tag{9}$$

and

$$\rho_e + \rho_\mu = \frac{1}{3}(2\rho_u - \rho_d - \rho_s). \tag{10}$$

The quark and lepton densities appearing in the last equation can be easily obtained from the derivatives of the total thermodynamical potential with respect to the corresponding chemical potentials.

The stellar matter phase diagrams associated with the sets of parameters under consideration are shown in Fig. 4. Comparing them with those corresponding to the symmetric matter case we observe that, in spite of an overall similarity, some differences arise. The first one is related to fact that the IMC is less pronounced in the present case. To understand why this is expected to be the case, let us start by reminding that this effect leads to a minimum critical

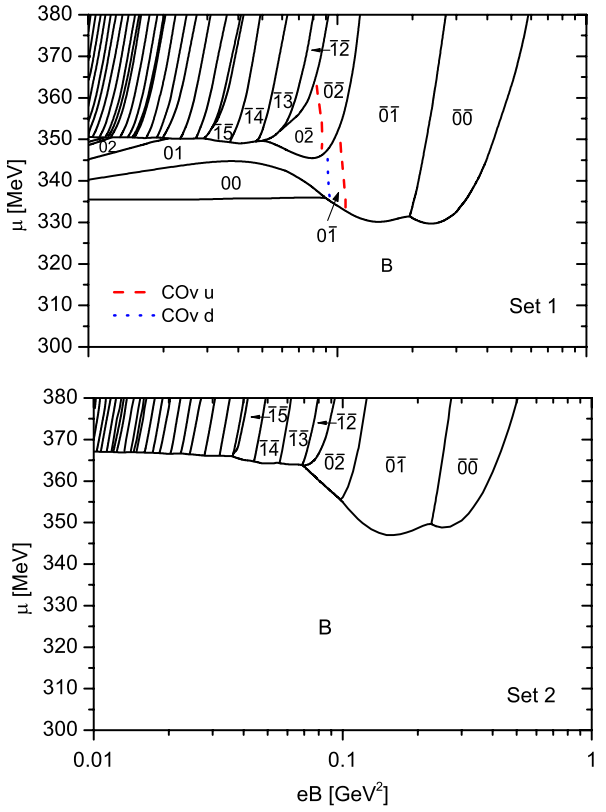

FIG. 4 (color online). Phase diagrams for stellar matter in the eB-μ for the set of parameters defined in Table I. As explained in the text, the pair of integers mn corresponds to the C_{mn} phase and the pair $\bar{m}\,\bar{n}$ to the A_{mn} phase. The case in which one quark is in a C-type phase and the other in the A-type phase is indicated by putting a bar on top of the integer associated with the A-type phase.

chemical potential at $eB \simeq 0.2$ GeV^2. As in the case of symmetric matter discussed in the previous section, in that region, the transition occurs between the B phase and an A-type phase in which the lowest LLL dominates. Generalizing to stellar matter the result found in Ref. [18]. one can show that, within the chiral limit approximation, the extra cost in free energy to form a fermion-antifermion pair at finite μ is proportional to $B\bar{\mu}^2$ with $\bar{\mu}^2 = \sum_f |q_f|\mu_f^2 + \mu_e^2/3$ and where an small muonic contribution has been neglected. Note that for the values of μ we are interested in, only the light flavors have to be taken into account. Thus, in what follows, $f = u, d$. Using the relations obtained from the β-equilibrium conditions, $\mu_f = \mu - q_f\mu_e$, we get $\bar{\mu} = \mu(1 - 2x/3 + 2x^2/3)^{1/2}$, where $x = \mu_e/\mu$. The minus sign in the (dominant) linear term follows from the fact that $|q_u| = 2|q_d|$. The relevant value of x follows from the neutrality condition Eq. (10). Assuming as before that in the A-phase we are dealing with massless quarks one obtains $x \simeq 0.38$ for $\mu \simeq 350$ MeV. Using this result, we get $\bar{\mu} \simeq 0.92\ \mu$. This implies that the extra cost in free energy is smaller than that required in the symmetric matter case for the same value of eB and μ. Consequently, for a given eB, one needs a larger value of the chemical potential to induce the phase transition. In fact, we have $\mu_c^{\rm st}/\mu_c^{\rm sym} \simeq 1.09$, a value that is in good agreement with our full numerical results $\mu_c^{\rm st}/\mu_c^{\rm sym} = 1.08(1.07)$ for Set 1 (Set 2), where the superindex st stands for stellar. Now, in order to determine which is the effect of the β equilibrium and charge neutrality conditions on the IMC effect, we have to analyze what happens at small values of eB. In fact, our numerical results indicate that in that region $\mu_c^{\rm st}/\mu_c^{\rm sym}$ is smaller than the value obtained at $eB \simeq 0.2$ GeV. To obtain an estimate of $\mu_c^{\rm st}/\mu_c^{\rm sym}$ at small values of eB, we can consider the limiting case $B = 0$. It is not difficult to show that the neutrality condition for massless particles in the chirally restored phase leads, in this case, to a third-order equation in x whose only real solution is $x = 0.22$. On the other hand, the extra cost in free energy induced by the chemical potentials is proportional to $\bar{\mu}'^4$ where $\bar{\mu}'^4 = \sum_f \mu_f^4/2 + \mu_e^4/6$. Expressing as before μ_f in terms of μ and x, we get $\bar{\mu}/\mu = 0.98$ for $x = 0.22$. Therefore, although we also expect that for small values of eB the critical chemical potential for stellar matter has to be larger than the one for symmetric matter (a feature confirmed by our numerical results), the estimated ratio $\mu_c^n/\mu_c^s \simeq 1.02$ is smaller than the one at $eB \simeq 0.2$ GeV, leading to a quenching of the IMC effect. From this discussion, we see that this is basically due to the smaller value of x as well as to the different form of the finite chemical potential free energy cost to create fermion-antifermion pairs at low magnetic fields as compared to that at values of eB where the LLL dominates.

The other significant difference between the symmetric and stellar matter phase diagrams concerns the A_α and C_α phases that can appear in each case. As discussed in the previous section, the relation between the light quark charges implies that for the rather strong flavor mixing considered in this work only phases with $m = \mathrm{Int}[n/2]$ are allowed. We see that for stellar matter this does not need to be the case. Again, this a consequence of the β equilibrium and charge neutrality conditions that lead to $\mu_u < \mu_d$. To see this more clearly, let us consider as an example the situation in which the system is the A_{01} phase and we increase the chemical potential keeping eB at a fixed value. For simplicity, we assume in what follows that the dressed quark masses are negligible. In the symmetric case, as one increases the chemical potential, at some point, there is a simultaneous population of the $\nu = 1$ u-quark and the $\nu = 2$ d-quark LLs leading to the transition from A_{01} phase to the A_{12} one. On the other hand, in the case of stellar matter the presence of a finite isospin chemical potential in the A-type phases opens the possibility of a sequential population of these LLs. Namely, since $\mu_u < \mu_d$, the $\nu = 2$ d-quark LL can be populated before that $\nu = 1$ u-quark LL, and thus, the transition from the A_{01} phase to the A_{02} one is possible.

Finally, one can see that, as in the case of symmetric matter, Set 1 leads to a richer phase structure than Set 2. In fact, the C-type phases are even more extended in the present case. Note as well, that in the case of Set 2, the crossover lines are not present in the phase diagram for stellar matter.

V. FINAL REMARKS

In the present work, we have revisited the phase structure of the magnetized cold quark matter within the framework of the SU(3) NJL model for two parameter sets often used in the literature [34]. We include in our analysis both symmetric and stellar quark matter.

For the symmetric case, although the general pattern is similar, the quantitative results are certainly parameter dependent, as in the case of the SU(2) NJL [25,26]. We have checked that Set 1, i.e., the one leading to lower vacuum values for the dressed quark masses in the absence of a magnetic field, presents a richer phase diagram, with more intermediate phases than Set 2. This is a reflex of the number of small jumps appearing in the quark dressed masses, which are related to the number of filled LLs. It is worth emphasizing that, different from the case of standard SU(2) NJL model with maximum flavor mixing studied in Ref. [26], within the present version of the SU(3) NJL model, the u- and d-dressed quark masses, as well as the corresponding condensates, are not necessarily equal for the same chemical potential μ and magnetic field B. As a consequence, three different susceptibilities (one for each flavor) can be defined that, in principle, might bear peaks at different points. This points toward the possibility of having a different crossover transition line for each of three quark flavors. In fact and in contrast to what happens with the first-order transitions which are always found to coincide, the results of our analysis indicate that for the parametrizations considered this is always the case. Hence, the corresponding phase diagrams turn out to have some (small) regions where the quarks of different flavor are in different phases.

The phenomenon of IMC as defined in Ref. [18]; i.e., the decrease of the critical chemical potential at specific values of the magnetic field intensity is clearly observed within the present choice of parameters for the SU(3) NJL model. In connection with this, we also note that the response of light quark dressed masses to an increase of the magnetic at fixed μ depends on the region of eB-μ phase diagram considered. On the one hand, the increase in light quark dressed masses with magnetic field, known as magnetic catalysis, is principally seen in the vacuum phase B, where chiral symmetry is fully broken. On the other hand, phases where some light quark levels are populated (C_i and A_i) show a dominant decrease in the corresponding masses as magnetic field increased.

Analyzing the case of the stellar quark matter, we found some differences respect to the symmetric one. First, when considering charge neutrality and β equilibrium we observed, as an overall effect, that in the corresponding phase diagrams, for both sets of parameters, the first-order phase transitions to the fully chiral restored phase are moved to higher chemical potentials. In particular, we found that this effect is larger for $eB \simeq 0.2$ GeV^2. As a consequence, the IMC phenomenon is less pronounced for the stellar matter case.

There is still another difference between the symmetric and stellar matter: we found that in the case of symmetric matter only phases with $m = \mathrm{Int}[n/2]$ are allowed, but when imposing charge neutrality and β equilibrium, the structure is somewhat different because in stellar matter the finite isospin chemical potential plays a role in the population of the LLs.

We conclude by pointing out that, in matter subject to magnetic fields, spatially inhomogeneous condensate configurations may be favored [35]. An important consequence of the possible existence of spatially inhomogeneous phases may considerably alter the currently most accepted picture of the QCD phase diagram at finite densities when, e.g., the critical end point would be replaced by a Lifschitz point as discussed recently in the literature [36]. In this sense, a detailed study of these phases in the context of the present $SU(3)$ NJL model would be of great interest. We should keep in mind, however, that even in the simpler case of the SU(2) model at $B = 0$ the effect of the finite current quark masses, which tends to reduce the size of these phases, has been only approximately taken into account so far [37]. In addition, the role played by the stellar matter conditions on the stability of these inhomogeneous phases also requires further clarification.

ACKNOWLEDGMENTS

This work was partially supported by CAPES, CNPq, and FAPESC (Brazil); by CONICET (Argentina) under Grant No. PIP 00682; and by ANPCyT (Argentina) under Grant No. PICT-2011-0113.

[1] K. Fukushima, D. E. Kharzeev, and H. J. Warringa, Phys. Rev. D **78**, 074033 (2008); D. E. Kharzeev and H. J. Warringa, Phys. Rev. D **80**, 034028 (2009).

[2] R. Duncan and C. Thompson, Astrophys. J. Lett. **392**, L9 (1992); C. Kouveliotou *et al.*, Nature (London) **393**, 235 (1998).

[3] D. P. Menezes, M. B. Pinto, S. S. Avancini, A. Pérez Martínez, and C. Providência, Phys. Rev. C **79**, 035807 (2009); D. P. Menezes, M. B. Pinto, S. S. Avancini, and C. Providência, Phys. Rev. C **80**, 065805 (2009); S. S. Avancini, D. P. Menezes, and C. Providência, Phys. Rev. C **83**, 065805 (2011).

[4] G. S. Bali, F. Bruckmann, G. Endrődi, Z. Fodor, S. D. Katz, S. Krieg, A. Schäfer, and K. K. Szabó, J. High Energy Phys. 02 (2012) 044.

[5] R. Gatto and M. Ruggieri, Lect. Notes Phys. **871**, 87 (2013).

[6] E. S. Fraga, Lect. Notes Phys. **871**, 121 (2013).

[7] K. Fukushima and Y. Hidaka, Phys. Rev. Lett. **110**, 031601 (2013).

[8] T. Kojo and N. Su, Phys. Lett. B **720**, 192 (2013).

[9] F. Bruckmann, G. Endrodi, and T. G. Kovacs, J. High Energy Phys. 04 (2013) 112.

[10] Y. Sakai, T. Sasaki, H. Kouno, and M. Yahiro, Phys. Rev. D **82**, 076003 (2010); J. Phys. G **39**, 035004 (2012).

[11] Y. Nambu and G. Jona-Lasinio, Phys. Rev. **122**, 345 (1961); **124**, 246 (1961).

[12] K. Fukushima, M. Ruggieri, and R. Gatto, Phys. Rev. D **81**, 114031 (2010).

[13] M. Ferreira, P. Costa, D. P. Menezes, C. Providencia, and N. Scoccola, Phys. Rev. D **89**, 016002 (2014).

[14] R. L. S. Farias, K. P. Gomes, G. Krein, and M. B. Pinto, arXiv:1404.3931; M. Ferreira, P. Costa, O. Lourenço, T. Frederico, and C. Providência, Phys. Rev. D **89**, 116011 (2014).

[15] V. A. Miransky and I. A. Shovkovy, Phys. Rev. D **66**, 045006 (2002).

[16] S. S. Avancini, D. P. Menezes, M. B. Pinto, and C. Providência, Phys. Rev. D **85**, 091901(R) (2012).

[17] P. Costa, M. Ferreira, H. Hansen, D. P. Menezes, and C. Providência, Phys. Rev. D **89**, 056013 (2014).

[18] F. Preis, A. Rebhan, and A. Schmitt, J. High Energy Phys. 03 (2011) 033; Lect. Notes Phys. **871**, 51 (2013).

[19] A. F. Garcia and M. B. Pinto, Phys. Rev. C **88**, 025207 (2013).

[20] R. Z. Denke and M. B. Pinto, Phys. Rev. D **88**, 056008 (2013).

[21] S. P. Klevansky and R. H. Lemmer, Phys. Rev. D **39**, 3478 (1989); H. Suganuma and T. Tatsumi, Ann. Phys. (N.Y.) **208**, 470 (1991).

[22] K. G. Klimenko, Theor. Math. Phys. **89**, 1161 (1991); Z. Phys. C **54**, 323 (1992); Nuovo Cimento A **107**, 439 (1994).

[23] V. P. Gusynin, V. A. Miransky, and I. A. Shovkovy, Phys. Rev. Lett. **73**, 3499 (1994).

[24] I. A. Shovkovy, Lect. Notes Phys. **871**, 13 (2013).

[25] D. Ebert, K. G. Klimenko, M. A. Vdovichenko, and A. S. Vshivtsev, Phys. Rev. D **61** (1999) 025005.

[26] P. G. Allen and N. N. Scoccola, Phys. Rev. D **88**, 094005 (2013).

[27] J.-L. Kneur, M. B. Pinto, and R. O. Ramos, Phys. Rev. D **88**, 045005 (2013).

[28] J. Randrup, Phys. Rev. C **79**, 054911 (2009); M. B. Pinto, V. Koch, and J. Randrup, Phys. Rev. C **86**, 025203 (2012).

[29] T. Hatsuda and T. Kunihiro, Phys. Lett. B **198** (1987) 126.

[30] J. L. Noronha and I. A. Shovkovy, Phys. Rev. D **76**, 105030 (2007); **86**, 049901(E) (2012); K. Fukushima and H. J. Warringa, Phys. Rev. Lett. **100**, 032007 (2008).

[31] T. Hatsuda and T. Kunihiro, Phys. Rep. **247**, 221(1994).

[32] P. Rehberg, S. P. Klevansky, and J. Hüfner, Phys. Rev. C **53**, 410 (1996).

[33] In fact, so it is χ_s, but since such a quantity never presents a peak for the values of eB and μ considered in this work, it will be ignored in what follows.

[34] M. Buballa, Phys. Rep. **407**, 205 (2005).

[35] I. E. Frolov, V. C. Zhukovsky, and K. G. Klimenko, Phys. Rev. D **82**, 076002 (2010).

[36] S. Carignano, M. Buballa, and B.-J. Schaefer, arXiv:1404.0057.

[37] S. Maedan, Prog. Theor. Phys. **123**, 285 (2010).